

## A Method for Assessment of the Survival Time of a Ship after Collision

Martin Schreuder

*Department of Shipping and Marine Technology Chalmers University of Technology, Sweden*

### ABSTRACT

Following an interdisciplinary calculation procedure, the chain of events of ship collision, flooding, and loss of stability within given time have been investigated. The method established in the current work concerns the interaction between structural and damage stability computations and has been used to study the influence of various parameters, e.g., significant wave height and size of damage opening on a RoPax-ferry damaged in a collision with a ship of similar size.

### KEYWORDS

Capsize, damage, flooding, RoPax-ferry, ship collision.

### INTRODUCTION

Collision and grounding constitute a significant part of ship losses in modern time (Lloyd's Register of Shipping 2000-2007). Thus, large research efforts are being put forth toward prevention and mitigation of the consequences of collision and grounding events through simulation. Being a complex problem, it involves numerous disciplines of research that traditionally have been treated separately with very limited interaction. The driving force concerning the development of regulations on maritime safety has traditionally been as a reaction to a major incident; rules have emerged afterwards in order to prevent it from happening again. However, in recent years, a tendency towards a more proactive and holistic approach in rule making has been seen, as with the latest SOLAS damage stability code that began to be enforced 2009 (MSC 2005). This code is the result of efforts made within the HARDER project which was completed in 2003. The aim of the project was to develop and implement a methodology for safety assessment and to evaluate its effect on both current and new ship designs. The development of damage stability codes is however a continuous process and the use of numerical methods in this process are likely to increase, see Vassalos and Jasionowski (2007) and Papanikolaou (2010).

Within the SAFEDOR project (Soares et al. 2009), a risk-based approach to ship design is suggested. It covers most aspects of the design process and suggests an approach on how to design in order to mitigate consequences of collision and grounding based on Monte Carlo simulations of damage scenarios. Vanem et al. (2007) also suggest a holistic and risk-based approach to collision damage stability by calculation of conditional probabilities of the sequence of events in a collision. In Simonsen et al. (2009), five fundamental challenges are suggested for doing full risk-based damage stability computations:

1. Define impact scenarios and their probability of occurrence.
2. Predict the damage, taking into account the impact scenarios and the structure of the vessel.
3. Predict the consequences of the damage in terms of e.g. loss of buoyancy, oil outflow, and loss of stability.
4. Assess whether the structural integrity is maintained or collapse will occur, possibly as a progression of local collapses leading to total loss.
5. Set acceptance criteria.

This investigation presents a methodology developed in a project in which the time to total

loss of a ship struck in a collision is established through a deterministic computational procedure. The methodology proposed in the current work focuses on the second and third issues in Simonsen's list of challenges (see above). The collision case studied is a RoPax-ferry struck amidships by a vessel of similar size. The shape and size of the damage opening in the struck ship are calculated by means of nonlinear explicit finite element analysis. Various collision events are assessed considering, among others, different speeds of the striking vessel and different locations of impact. Further on, dynamic stability simulations of the damaged (struck) ship in various sea states are presented. The influence of significant wave height, the wave spectrum, and also the heading of the vessel relative to the waves are studied. The influence from wave direction in damage stability calculations has also been studied by Lee et al. (2007).

#### DESCRIPTION OF METHODOLOGY AND A CASE STUDY

In this investigation, a comprehensive calculation procedure has been developed that is useful for quantitative assessment of the survivability of damaged ships. It incorporates the analysis of structural collision resistance, structural stability and collapse, and time simulation of ship flooding and stability in waves. The connection and interaction between nonlinear structural damage analysis and seakeeping/stability is unique, i.e. to handle the entire system with a particular focus on chain of sequences and consequences that may pose a risk to the survivability of a struck ship. The calculation procedure is implemented in existing numerical simulation tools.

The work presented in this investigation was carried out within the project HASARD (Holistic Assessment of Ship Survivability and Risk after Damage). Its main objective is to outline a comprehensive calculation procedure that can quantitatively be used for the assessment of damaged ship survivability, incorporating structural collision resistance as well as ship flooding and stability in waves. One of the aims of the project is to contribute to IMO's late efforts in the development of a holistic and risk-based approach of assessing the consequences of damages of ships and the mitigation of these. A

step towards accomplishing this is through deeper insight and understanding of the mechanisms governing the collision impact and further development of phenomenological models in, for example, structure and damage stability analyses.

#### *Calculation procedure*

The calculation procedure constitutes two tracks: structure and stability. Deliverables from the structure track include, among others, phenomenological models, which, with satisfying reliability, can mimic the collapse and rupture phenomena in ship-to-ship collision simulations using the finite element (FE) method. Deliverables from the stability track include further enhancement of the SIMCAP computer code (Schreuder 2005) developed for the analysis of transient ship instability conditions and a formulation of procedures that may quantify the ability of a damaged ship to stay upright. The SIMCAP computer code used in the stability track has recently been validated and successfully used in the research study on the sinking sequence of the M/V *Estonia* (Schreuder 2008). The code was also validated for the ship used in the present study in Schreuder (2005), following the benchmark study in ITTC (2002), see Figure 5.

The two tracks of the project operate in close collaboration through the exchange of information, which leads them towards a common aim: to develop a calculation procedure for becoming a useful tool for risk analysis (structural collapse and ship stability) of the survivability of a collided and flooded ship. Figure 1 gives a schematic representation of an iterative procedure between tracks. The collision event is discretized in time to enable the transfer of information between models, such as collision damage pattern, ship flooding and stability in waves, and global and local loads acting on the structure.

Due to the complexity of the numerical models in the structure track, laboratory experiments and experiences from FE simulations are valuable for the validation of some of the models and calculation procedures, especially regarding collision impact, energy absorption, material rupture and damage pattern (Hogström et al. 2009 and Karlsson et al. 2009). These necessary tests determine material and structural characteristics for a loading situation similar to

that of a ship-to-ship collision event. Figure 2 illustrates the range in scales in material testing and numerical simulation of a ship collision and grounding.

focus of this paper is however on the stability analysis and a summary of all of the numerical simulations carried out in the stability track is presented in Table 1.

In the following sections, the structural and stability analyses are described in more detail. The

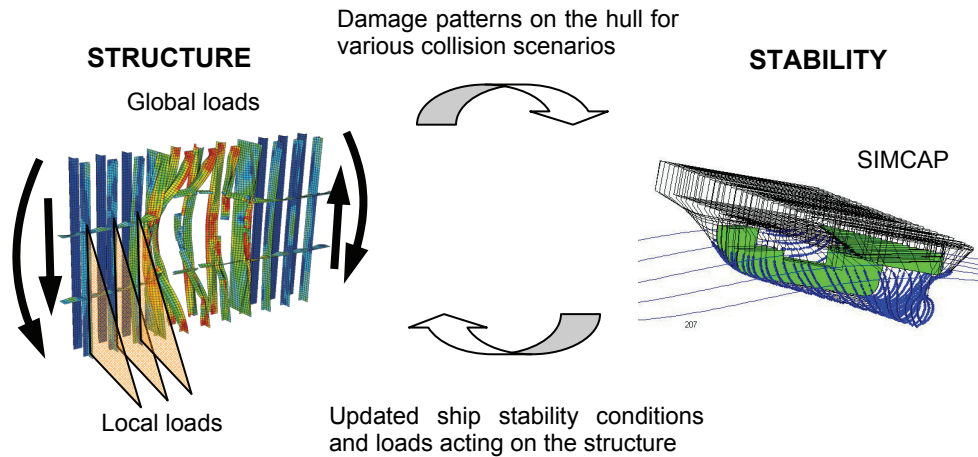


**Fig. 1: Iteration scheme between structure and stability tracks. The structure track delivers the damage pattern caused by the collision to the stability track, which calculates the ship's behaviour in the damage situation. There is also a possibility to update the load condition in the structure model and thus create a feedback loop between the two tracks.**

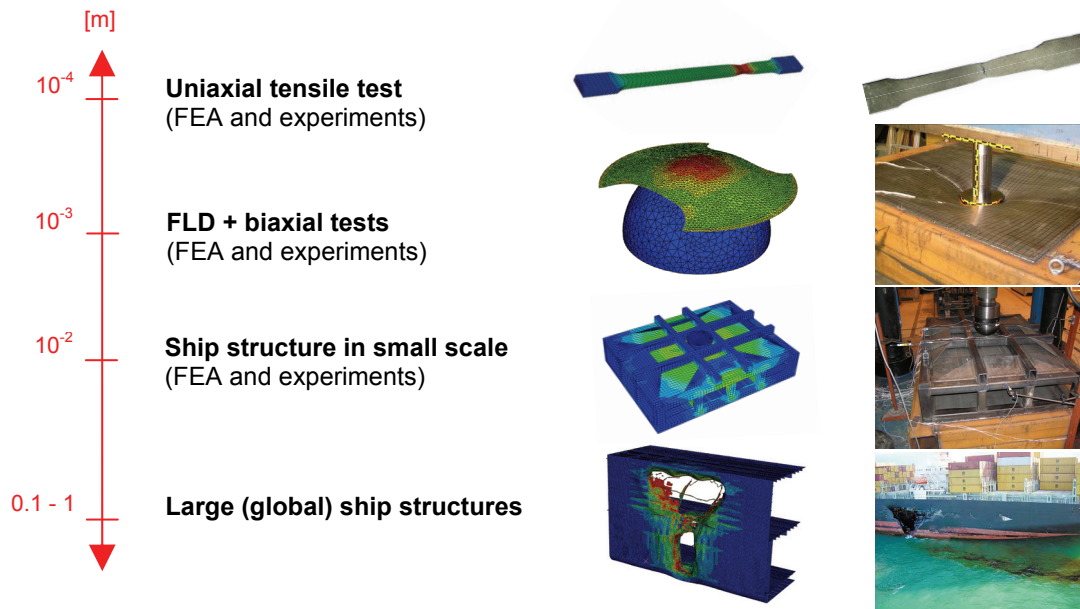


**Fig. 2. Illustration of range in scales (approx. resolution in FE mesh) in material testing and numerical simulation of a ship collision and grounding**

**Table 1. Damage stability simulations using the SIMCAP code.**

Parameter	Convergence study		Collision survivability		Parameter sensitivity analysis	
	Quantity	Value	Quantity	Value	Quantity	Value
Wave spectrum	-	No waves	2	Jonswap/P-M	1	Jonswap
Wave height	-	-	11	3-8 m	5	3.0-5.0 m
Spectrum seed	-	-	8	Random	50	Random
GM	1	12.89 m	3	12.89±1 m	1	12.89 m
Heading	-	-	16	0°-360°	1	Following seas
Damage	3	2.5-39 m <sup>2</sup>	2	1-2 compartment	1	2-compartment
Position	3	3-6 m (from KL)	2	-	1	-

### Description of a case study

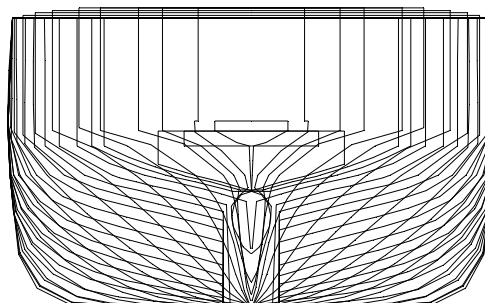
A case study of a ship-to-ship collision of a RoPax-ferry was carried out. The main particulars and hull lines of the struck ship are presented in Table 2 and Figure 3. The case study is comprised of two damage cases corresponding to SOLAS one- and two-compartment damages (IMO 1997), see Figure 4. The SIMCAP code has previously been validated for the two-compartment damage case regarding hydrostatic properties and response amplitude operator, see Figure 5 and further Schreuder (2005) and ITTC (2002). The damage cases are subjected to different damage case configurations reflecting the circumstances at the time of the collision event, specifically damage opening, loading condition (vertical center of gravity, KG), ship heading, wave spectra and wave height. The influence of the natural variation in the sea state is studied by realisation of eight different irregular wave trains where only the phase angles between wave components are changed as random numbers with uniform distribution from 0 to  $2\pi$ . In Resolution 14, Annex 5 in IMO (1997), at least five realisations are stipulated for model tests, similar to the simulations presented in this investigation.

Both damage cases are results of the ship being struck amidships by a similar sized ship at a 90° angle of attack. In the one-compartment damage case, only the vehicle deck and the void space (void) can be subjected to flooding, and the damage case is symmetric. In the two-compartment damage case, however, four different spaces can be subjected to flooding: the vehicle deck, the starboard heel tank (SB htk), one

machinery space (mach) inside of the heel tank, and the void space forward of the heel tank, see Figure 4. This damage case is asymmetric with a list angle of approximately 3 degrees at static equilibrium, and it corresponds to the worst SOLAS damage (IMO 1997).

**Table 2. Main particulars of the RoPax-ferry.**

Particulars		
Length over all, $L_{OA}$	179	m
Length, $L_{pp}$	170	m
Breadth, B	27.8	m
Draught, T	6.25	m
Depth, $D_{cardeck}$	9.00	m
Displacement, $\Delta$	17300	tonnes
Center of gravity, $KG_{intact}$	12.89	m
Metacentric height, $GM_{intact}$	2.63	m


**Fig. 3. Hull lines of the PRR01 RoPax-ferry.**

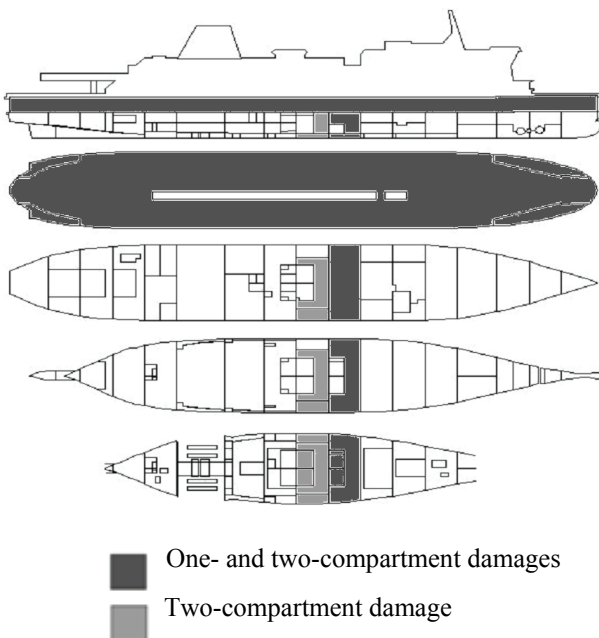


**Fig. 4. The RoPax-ferry with the damaged compartments shaded.**

### DAMAGE OPENING COMPUTATIONS

The structural computations of shapes and sizes of damage openings of the struck ship were carried out using the commercial FE code Abaqus/Explicit (Dassault Systèmes 2007). In the FE analyses, a bulbous bow impacts with and penetrates a ship hull structure, a scenario that has been studied for different impact speeds of the striking bow. The resulting structural damage in the hull, and specifically the shape and size of the resulting damage opening, are calculated. The damage opening is then used in subsequent stability investigations, which are detailed in the following two sections.

The FE analyses are restricted to the internal mechanics during the collision. The ship structure struck in the collision is held fixed while the striking ship is given an initial kinetic energy, which gradually decreases during the collision event as energy is dissipated plastically and as fracture develops in the hull structure. The elasto-plastic material model is combined with a failure model, which eventually brings the material in the FE model to fracture through element erosion. The failure model involves a criterion for damage

initiation and a damage evolution law. External dynamics could have given further information about the fraction of kinetic energy that is dissipated in other ways than in the structure, for instance through added mass effects, wave making and viscous effects; however, this is not a focus in the current study.

### DAMAGE STABILITY SIMULATIONS

The simulation and analysis of stability of damaged ship were carried out using the SIMCAP programme (Schreuder 2005). It is based on nonlinear strip theory in which the incident wave forces, the Froude Krylow forces, are calculated by integration of dynamic wave pressure over the momentarily wetted hull surface at each time step. Weight and inertial forces from water inside the damaged compartments are also derived in each time step. In a simulation without waves all static stability properties are represented in the code.

In SIMCAP, the floodwater surface is always considered to be horizontal, and sloshing is not accounted for. Diffraction and radiation forces are based on pre-calculated sectional hydrodynamic coefficients. Roll damping can be treated linearly or non-linearly depending on whether test data is available. In the current case, linear damping was used. The damage opening is modelled by a number of grid points, and each is associated with an area. The inflow or outflow of water in a grid point is determined by its location and area by use of the Bernoulli's equation; see Schreuder (2005) for details. In the present investigation, in order to have a realistic representation of the shape and size of the damage opening, the grid points were determined accurately by means of FE analysis. See Figure 6 for an illustration of this. The flood rate through the damage opening is the sum of the flood rates through each point.

The adopted damage opening definition with a fixed grid of points is favourable with respect to computation time and robustness; but, an appropriate minimum resolution of the grid must be established. For this purpose, a convergence study was carried out with a systematic variation of damage opening size, position and resolution for a single damage case.

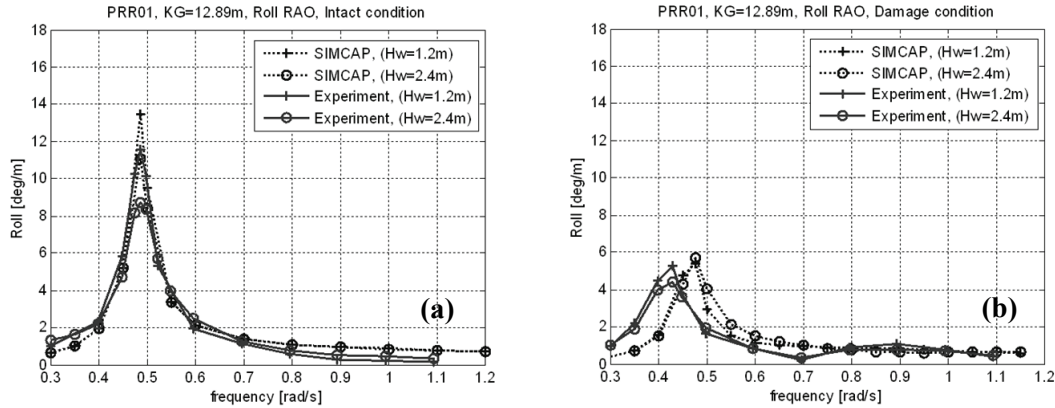


Fig. 5: Experimental and numerical roll response amplitude operator (RAO) of the RoPax-ferry for two wave heights (Hw), see Schreuder (2005): (a) RAO for intact ship, and (b) the two-compartment damage.

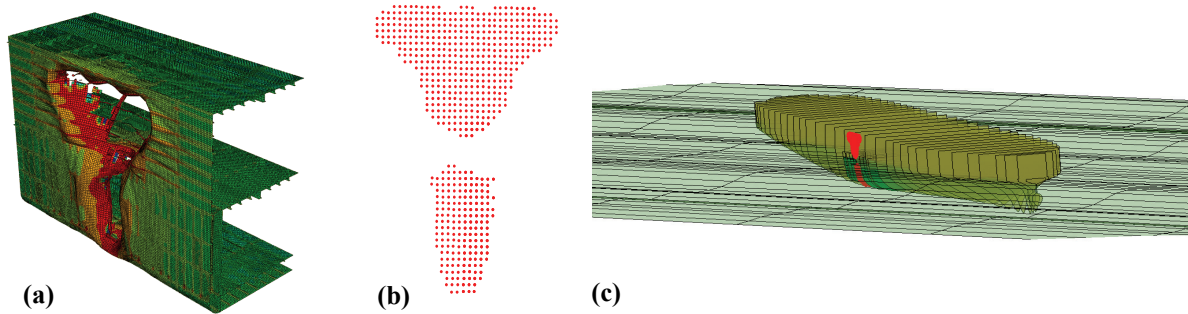


Fig. 6: (a) Structural damage and damage opening from FE analysis; (b) illustration of representation of damage opening by grid (area) points used for flooding calculations; (c) illustration of damaged ship in a seaway.

### Convergence study using SIMCAP

A convergence study using SIMCAP was carried out in order to determine the lowest required resolution that is needed to represent the damage opening in the SIMCAP code. The convergence study was carried out considering five different resolutions in conjunction with the influence of the resolution on the size and position of the damage opening. The configurations incorporated into the study are presented in Table 4.

In the convergence study, a RoPax-ferry with a one-compartment asymmetric damage was utilized. The damage opening was always below the bulkhead deck near amidships. For simplicity in the convergence study, the openings were generated by FE analysis using a half-sphere indenter as the bulbous bow for penetration of the struck hull. The damage configurations, shown in

the first column of Table 2, were simulated using SIMCAP in still water, but some reference simulations in a seaway were also made. Figure 7 shows the ship at the final static equilibrium of the damage case studied in the convergence analysis.

Figure 8 shows the damage opening sizes and vertical positions for the resolution case #3. All damage openings, except for the lowest resolution in which the opening was modelled with only one point, were geometrically similar. Figure 9 shows the time series of the simulations of the 27 original damage case configurations in calm water. The configurations consist of a variation of three sizes, three positions and three resolutions. The level of convergence was estimated by comparing the time series of roll motion and volume of flooded water for different resolutions.

**Table 3. Damage opening parameters**

Resolution		
#1	1	point
#2	157	points
#3	571	points
(#4)	2189	points)
(#5)	8572	points)
Size		
L (1:1)	39.25	m <sup>2</sup>
M (1:2)	9.81	m <sup>2</sup>
S (1:4)	2.45	m <sup>2</sup>
Position (centre of opening from keel line, KL)		
Lower	3	m
Middle	5	m
Upper	6	m

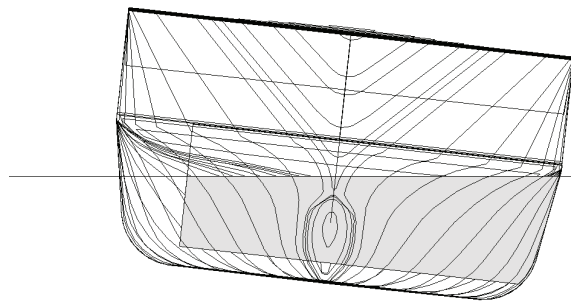


**Fig. 7. Ship at final static equilibrium.**

There is an almost ideal agreement among the different resolutions of the damage case configurations; in fact, the curves are almost overlapping, and the differences can not be seen in Figure 9 (b) and (c). The only exception is the small damage opening in the upper position where the time series for resolutions #2 and #3 are clearly separated. This resolution dependence of the upper vertical position is due to the fact that only a small portion of the damage opening is initially below the water surface, and the low flood rates in the first half of the simulation are affected by the resolution. Note that there is no flooding for resolution #1 in this case since the

damage opening is above the water line. Simulations in waves for the same damage case configuration, however, show a reasonable convergence, which can be seen in Figure 10. Additional refinement in resolution (#4 and #5 in Table 4) as well as lowering the damage opening in small increments also shows converging results

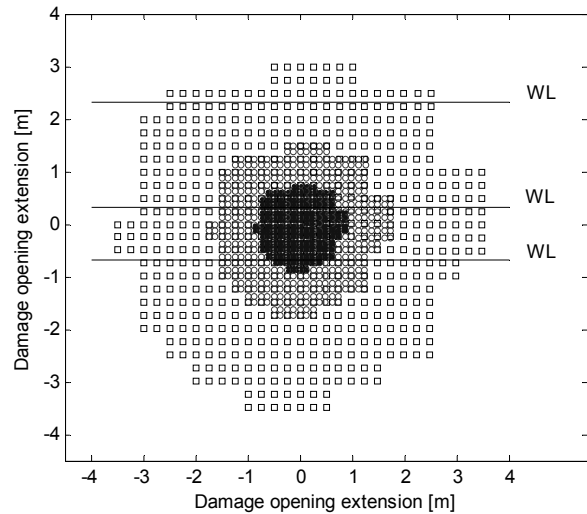


**Fig. 8. Damage opening size (resolution #3) and vertical positions (WL = water line).**

The result of the study shows that most of the cases are independent of the resolution. The limiting case occurs when only a small portion of the damage opening is below the surface. The dependence of opening resolution is smaller in the presence of waves. Resolutions used in the following studies were governed by the need for an accurate geometric description of the damage openings, which were generated by the FE computations with a homogenous opening grid.

**CASE STUDY: ANALYSIS OF COLLISION SURVIVABILITY OF A ROPAX-FERRY**

The aim of the collision survivability study is to investigate the behavior of a ship after a collision that has resulted in a breach of the water tight integrity. The study is mainly focused on ship capsizes, specifically the time interval from collision to capsizes,  $T_{cap}$ , which is strongly but not exclusively linked to the available time for evacuation of the ship. This is explained below along with the definition of ship capsizes.

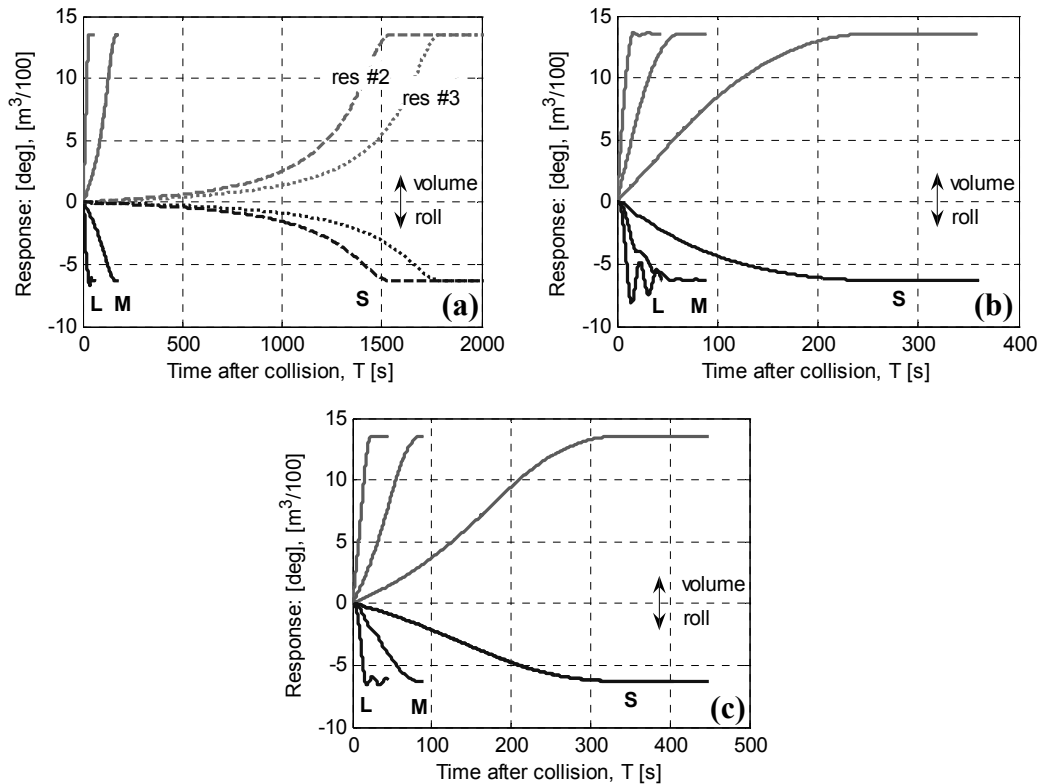


**Fig. 9:** Time series of the original 27 simulations in the convergence study for the three different positions: (a) lower, (b) middle and (c) upper. Shown are the ship roll response (lower curves) and flooded volume (upper curves). Three sizes of the damage opening: small (S), medium (M) and large (L), as well as three different resolutions, #1, #2 and #3, see Table 4. Note that results from different resolutions in (b) and (c) overlap.

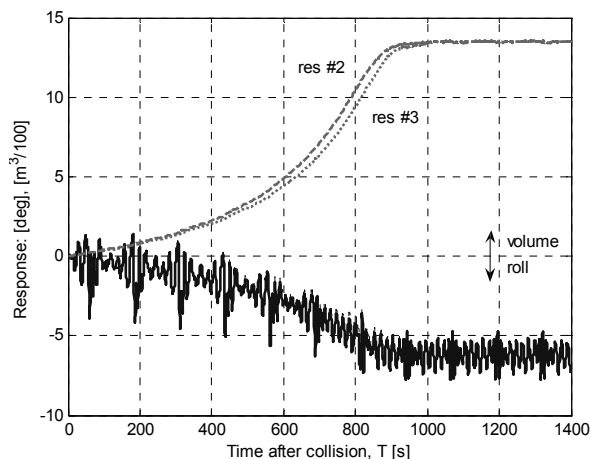


**Fig. 10:** Response and water flow for simulation in waves with small damage opening in upper position.

The struck ship used in the case study is the PRR01 RoPax presented above and the simulations are summarized in the middle column of Table 2. In static conditions or in moderate sea states, the two-compartment damage case would

not be fatal from a stability point of view. However, in more severe sea states and with a large damage opening to the vehicle deck made by the upper bow of the striking ship, accumulation of water due to wave action will occur and finally capsize of the ship. Also, the capsize mode of the two damage cases is of quasi-static nature, i.e. capsize is essentially governed by the amount of floodwater on the vehicle deck. This capsize mode has been recognized in model tests (Tagg and Tuzcu 2003), and it is typical for ships with large open vehicle decks.

Figure 11 shows an example of a time series of a SIMCAP simulation which resulted in ship capsize after 324 s. The qualities of this time series are typical for a capsize simulation, i.e. there is a fairly slow development of list and accumulation of floodwater on the vehicle deck followed by a very rapid capsize process, from about 30° to 180° of list. This rapid process can partly be explained by the absence of a superstructure, and hence buoyant volumes, of the

hull model in the simulations. However, a non-watertight superstructure cannot prevent capsize; it can only slow down the process towards an inevitable event (Schreuder 2008).

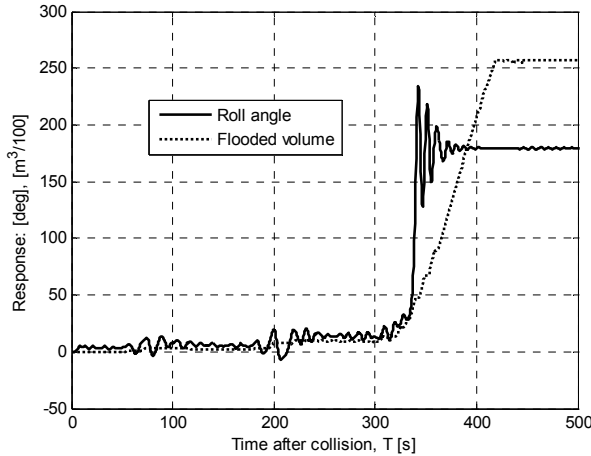


Fig. 11. Time series of typical capsize simulation.

### Assumptions and Conditions Used in the Numerical Simulations

It is assumed that there is no flooding during the collision event simulated by the FE analysis. There is no water in the floodable spaces at the beginning of the SIMCAP damage stability simulations, and it is assumed that the striking ship is not obstructing the damage opening.

The time to capsize,  $T_{cap}$ , is defined as the time when the floodwater volume on the vehicle deck reaches  $2000 \text{ m}^3$ . The list of the ship is now approximately  $25^\circ$ . Beyond this angle, evacuation of the ship would be very difficult, and the absence of superstructure in the ship model would also make the simulation unrealistic. This definition of  $T_{cap}$  will be simple and robust since the floodwater volume is monotonically increasing above about  $1800 \text{ m}^3$  as opposed to, for example, the fluctuating roll angle. The ship will always capsize, i.e. it will reach a roll angle of  $180^\circ$  within a few wave encounters after this amount has been reached.

A dead ship condition with no forward speed is assumed in all simulations. The duration of each simulation is 1800 s. The spaces below the vehicle deck will flood very rapidly after the start of the simulations. They will be flooded to the mean outside water level after about three minutes,

regardless of the wave height, a typical example of which can be seen in Figure 12. There will be only small volume fluctuations during the rest of the simulations. The floodwater weight, inertia, and the developed free surfaces will directly influence the behavior of the ship, but this influence is not affected by any of the studied parameters.

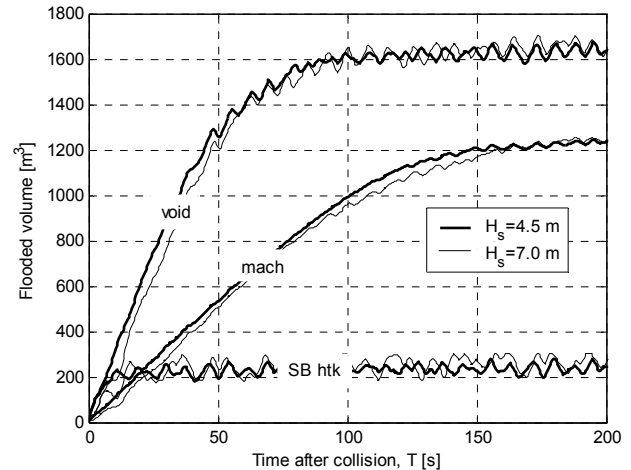


Figure 12. The flood rate of the spaces below the vehicle deck is independent of wave height.

### Results: Capsize Probability

A first set of simulations were made in order to investigate the influence of ship heading. These simulations were made for the two-compartment damage and with a loading condition corresponding to  $KG = 12.89 \text{ m}$ . The sea states were represented by two different energy density spectra: Jonswap with a peak period  $T_p = 4 \cdot \sqrt{H_s}$  and a peak enlargement factor  $\gamma = 3.3$ , and Pierson-Moskowitz (P-M) with  $T_p = 12 \text{ s}$ . The significant wave height ( $H_s$ ) ranged from 3 to 8 meters, with an increment of 0.5 m. Eight different headings were used (one every  $45^\circ$ ). For the Jonswap spectrum, an additional eight headings were simulated (one every  $22.5^\circ$ ). In addition, the wave elevation of the realisation of an irregular wave along the wave direction,  $x$ , can be described as:

$$\zeta(t) = \sum_{i=1}^n a_i \cos(k_i x - \omega_i t + \varepsilon_i) \quad (1)$$

where, for wave component  $i$ ,  $a_i$  is the amplitude,  $k_i = 2\pi/\lambda_i$  where  $\lambda_i$  is the wave length,  $\omega_i = 2\pi/T_i$

where  $T_i$  is the wave period, and  $\varepsilon_i$  is the phase. The amplitudes  $a_i$  are defined from the spectrum under consideration (here, either the Jonswap or the Pierson-Moskowitz spectrum) as  $a_i = \sqrt{2S(\omega_i)\Delta\omega}$ , where  $S(\omega)$  is the spectrum and  $\Delta\omega$  is the distance between the discrete wave components of the realization. The phases  $\varepsilon_i$  are random numbers which have uniform distribution from 0 to  $2\pi$ .

To account for the natural variation in sea state during testing in a laboratory environment, IMO (1997) recommends that at least five different irregular waves should be compared by random variation of the phase shifts  $\varepsilon_i$ . The recommendation was followed in the current investigation where one irregular wave realization is referred to as a “wave seed”; note, eight wave seeds were used in current investigation for each damage case.

The time to capsize is collected from the time series of all simulations. In Figure 13,  $T_{cap}$  is plotted against the significant wave height for one heading of the Jonswap spectrum simulations to provide an example. The traces from the eight wave seeds are plotted (data at  $T_{cap} = 1800$  s means that there was no capsize at the end of the simulation run). The appearance of the traces of the different wave seeds suggests the existence of a survival limit within the simulation time of 30 minutes, i.e. a wave height below which capsize is unlikely to occur for the simulated sea state conditions; see also e.g. Spanos and Papanikolaou (2007). This corresponds to a steady state floodwater volume (below  $\sim 2000$  m<sup>3</sup>) on the vehicle deck. Note that for sufficiently small individual waves, the vehicle deck will not be flooded due to the residual freeboard.

The area enclosed by the traces in the graph of Figure 13 constitutes a capsize band (Jasionowski et al. 2003), i.e. the probability of capsize increases within the band as the wave height or time increases. This is exemplified in Figure 14 in which the cumulative probability of capsize versus  $T_{cap}$  is plotted for significant wave heights 4.0 m, 4.5 m and 5.5 m, based on data from the parameter sensitivity analysis described below.

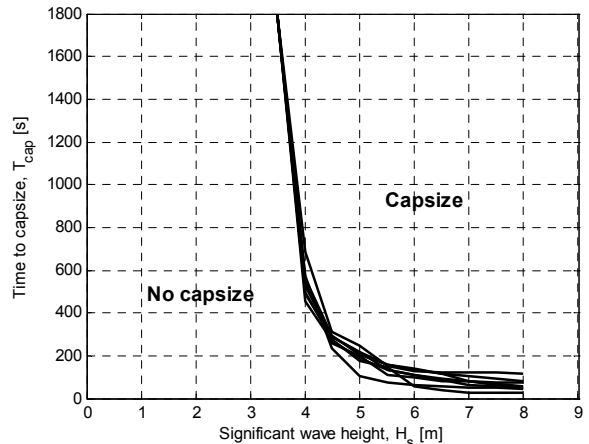


Fig. 13: Capsize band from 8 wave seeds of following seas simulation with Jonswap spectrum.

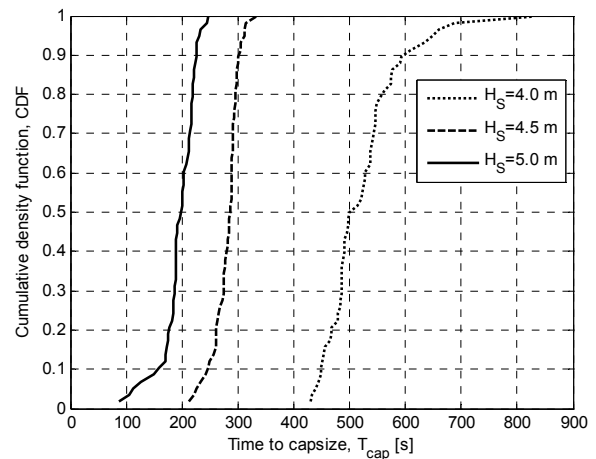


Fig. 14 Cumulative density functions of capsize probability versus  $T_{cap}$  for  $H_s = 4.0$  m, 4.5 m and 5.0 m.

### Results: Influence from Heading Angle and Significant Wave Height on $T_{cap}$

In Figure 15 the mean values of  $T_{cap}$  from the different wave seeds are plotted on the radial axes of polar plots, which aggregate all results from the first simulation set. In the mean value calculation,  $T_{cap}$  exceeding 1800 s have been truncated to 1800 s. The results show that the worst heading is beam seas onto the damage opening and quartering seas on the opposite side of the damage, regardless of wave height and for both the Jonswap and P-M spectra. They also show that the safest heading would be with the waves on the bow onto the damage opening. All capsizes in this simulation set occurred towards the damage, the side with the lowest righting levers

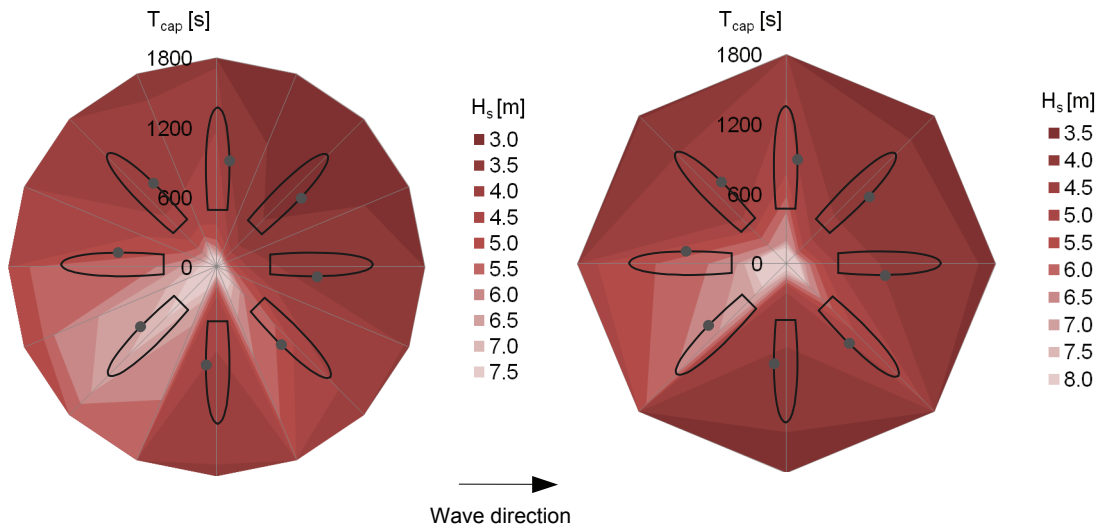


Fig. 15: Polar plots of the results from the Jonswap (left) and P-M (right) simulations. The color scale corresponds to  $H_s$  and mean value of  $T_{cap}$  is on the radial axis. Wave direction is from left to right and the damage opening is marked with a dot

**Results: Influence from KG on  $T_{cap}$**

In the next simulation set only beam seas with the damage opening towards the waves is simulated for the one-compartment damage case. Figure 16 shows the lower capsizes band envelope for different loading conditions (KG values).

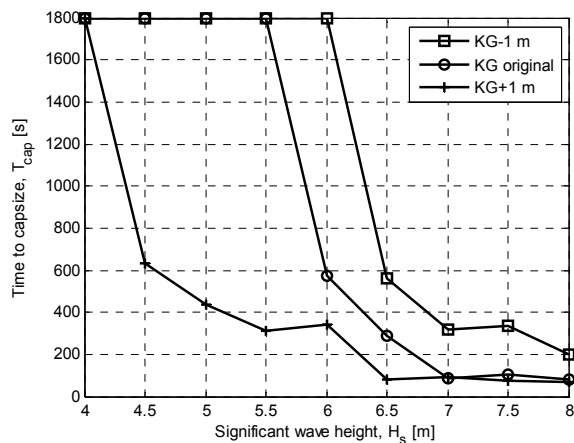
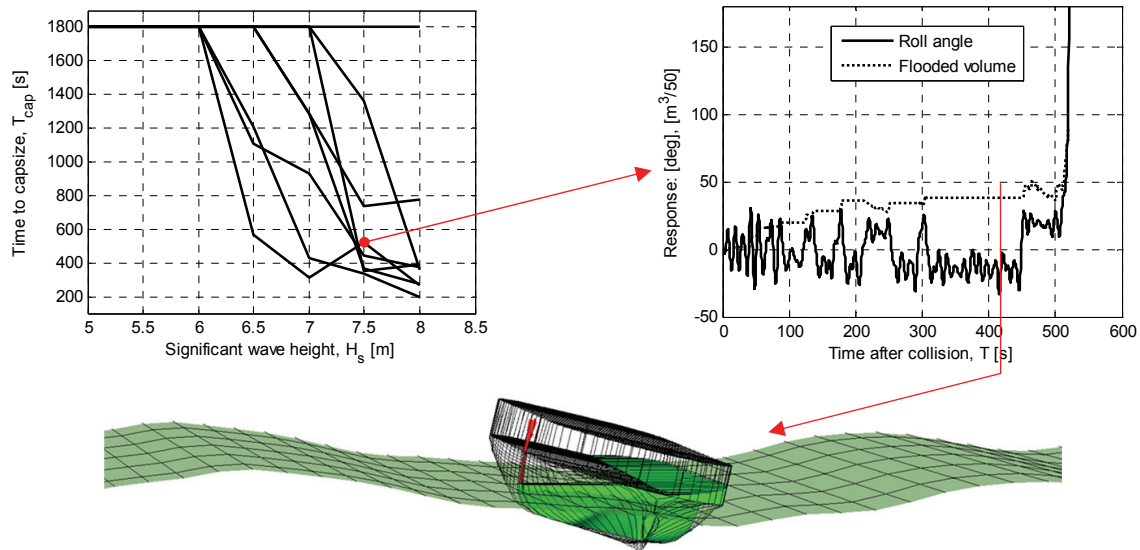


Figure 16. Lower capsizes band envelope of capsizes bands for different values of KG.

The loading conditions correspond to intact GM values of 1.63 m, 2.63 m and 3.63 m, respectively. The capsizes resistance or survival limit is drastically lowered as KG increases.

Because the damage case in this simulation set is symmetric, it is not evident that a possible capsizes will be towards the damage (here also towards the waves). However, out of 115 capsizes, only one occurred towards the opposite side. This is because the freeboard at the damage is significantly increased as the ship is heeling away from the damage, which slows down or cancels the flooding process. In connection to this, at the early stages of flooding of the vehicle deck each wave shifts the ship between starboard and port equilibrium; the static upright GM is always negative when there is water on the vehicle deck. As the floodwater volume increases, the ship heels to either side as the energy needed to shift the ship becomes increasingly larger. In some cases the ship gets stuck with a list away from the damage, with no in- or outflow of water, for several minutes until the right wave train is able to shift the ship back again, as depicted in Figure 17. It is believed that this behaviour is quite complex and random in nature and can explain the irregular appearance in, e.g., the marked trace in the upper left graph of Figure 17. For this simulation,  $T_{cap}$  has been significantly increased due to the port side heel during which the floodwater volume is constant as described above.



**Fig.17:** The left graph shows the capsize band of a damage case configuration. The red dot denotes a simulation which time series is shown in the right graph. Here, the ship got stuck with a list away from the damage for about two minutes (the below picture is a snap shot from simulation at time = 418 s) and  $T_{cap}$  is increased accordingly.

### PARAMETER SENSITIVITY ANALYSIS

In the collision survivability study following the SOLAS regulation for model tests (IMO 1997), 8 different wave seeds were simulated for each set of damage case configuration in order to capture the natural variation in the sea state. But, the results presented in Figure 13 shows that the 8 wave seeds result in a variation in the time to capsize,  $T_{cap}$ . Then, one can ask whether 8 simulations are sufficient or not? (Obviously,  $T_{cap}$  depends on sea state parameters and the type of damage, hence, the sensitivity analysis has been performed in respect of dependence on  $T_{cap}$  of the parameters). Often only the expected time to capsize is of interest. However as can be seen in Figure 13,  $T_{cap}$  depends also on sizes and order of random waves. This variability is of interest by its own. Consequently, the variability in  $T_{cap}$  is most conveniently described by probability distribution or some moments, e.g. coefficient of variation. Therefore, 50 additional wave seeds were simulated for 5 different wave heights; see Section 5.2 for details with regard to definition of a wave seed in the current investigation. Figure 18 shows the original and additional wave seed simulations. The additional 50 wave seed simulations were made for wave heights ranging

from 3.0 m to 5.0 m, whereas the original 8 wave seed simulations continued up to 8 m.

The results in Figure 18 suggest that the scatter in  $T_{cap}$  for the 58 simulated wave seed configurations must be investigated further, such as, if eight wave seeds are sufficient or if a larger number of them must be simulated. Hence, in Figure 19, the mean value and standard deviation of  $T_{cap}$  are plotted against the number of simulation runs (maximum: 58) for the wave heights 5.5, 6.0 and 6.5 m. The left column shows the “original simulation order” where the simulations,  $s$ , were ranked as  $s = \{s_1; s_2; s_3; \dots; s_{58}\}$ ; this is denoted as “1 permutation” in the figure. The results in this column show that the mean value and standard deviation of  $T_{cap}$  have converged after some 40 simulations (wave seeds). The simulations,  $s$ , are independent and the order in which they appear in a simulation sequence affects the mean value and standard deviation of  $T_{cap}$  when the number of simulations is smaller than 58. Thus, the confidence interval of the original simulation was estimated numerically by permutation of the order of the simulations in the calculation of the mean and standard deviation values. The middle column in Figure 19 shows the trend after 10 permutations,

and the left column after  $10^4$  permutations which was deemed sufficient for the analysis.

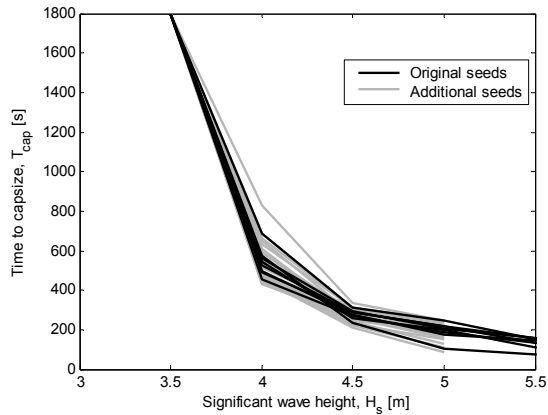


**Fig. 17: Time to capsize,  $T_{cap}$ , versus significant wave height,  $H_s$ . Illustration of the variation in  $T_{cap}$  due to different wave seed configurations for one collision scenario**

The mean value and standard deviation of  $T_{cap}$  for the  $10^4$  permutation analysis were calculated at 8 simulations and compared with the values at 58 simulations. Here, the mean value and standard deviation of  $T_{cap}$  at 58 simulations are assumed to

be accurate. In Table 5 these values are compared with the corresponding values at 8 simulations together with the standard deviation of the same values at 8 simulations.

## DISCUSSION AND CONCLUSIONS

In this investigation an interdisciplinary calculation procedure is presented in which the chain of events of ship collision, flooding, dynamic stability assessment and time to capsize is investigated. A robust damage opening definition allowing for the complex damage pattern that can be expected from a collision impact was developed. Results from the convergence study show that the resolution of the damage opening can be kept quite small as long as the boundary of the opening is represented correctly. One specific case in which relatively high resolution was needed in the calm water simulation was identified. However, this demand on resolution was not present for a corresponding simulation in a seaway.

**Table 5. Statistical error using 8 seeds compared to using 58 seeds.**

$H_s = 4.0$ m	
mean error of mean value	<0.1% (mean of 58 simulations: 523 s)
standard deviation of mean value	23 s (4%)
mean error of standard deviation	7.8% (standard deviation of 58 simulations: 71 s)
standard deviation of standard deviation	28 s (39%)
$H_s = 4.5$ m	
mean error of mean value	<0.1% (mean of 58 simulations: 280 s)
standard deviation of mean value	8 s (3%)
mean error of standard deviation	5.1% (standard deviation of 58 simulations: 23 s)
standard deviation of standard deviation	7.2 s (31%)
$H_s = 5.0$ m	
mean error of mean value	<0.1% (mean of 58 simulations: 195 s)
standard deviation of mean value	10 s (5%)
mean error of standard deviation	7.2% (standard deviation of 58 simulations: 32 s)
standard deviation of standard deviation	11 s (34%)

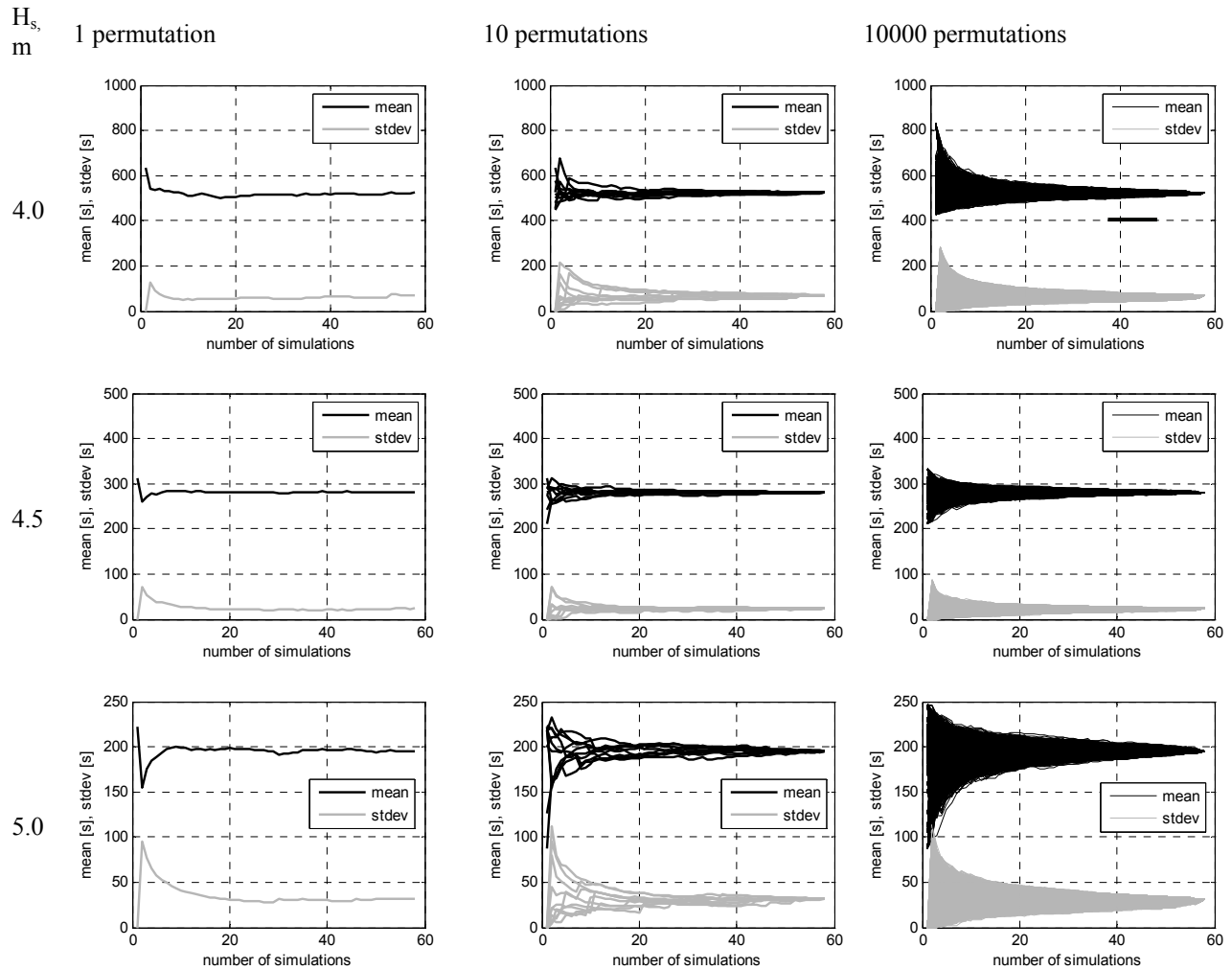


Fig. 19: Evolution of mean value (mean) and standard deviation (stdev) of  $T_{cap}$  as the number of simulations increases. Original simulation order (left). Ten random permutations (middle).  $10^4$  random permutations (right).

In the collision survivability study capsizing boundaries were produced by collecting the time to capsize,  $T_{cap}$ , from simulations with different wave seeds and with varying wave heights,  $H_s$ . The qualitative nature of these capsizing bands corresponds with the expected results, i.e. the existence of a limit wave height below which capsizing will not occur (or occur only with a low probability) was demonstrated as well as the steady decrease of  $T_{cap}$  as the wave height increases. Furthermore, capsizing bands were produced for different ship headings and wave spectra, P-M and Jonswap, and the mean value of the capsizing bands, i.e. mean value of  $T_{cap}$  for the different wave seeds, were presented in polar plots

(see Figure 15). These plots show that the most severe heading is beam and quartering seas for both wave spectra, whereas the least severe heading is bow waves with the damage opening onto the waves.

The capsizing bands can also be represented by cumulative density functions of  $T_{cap}$  for different wave heights, as is exemplified in Figure 14 which, e.g., shows that the probability of capsizing within 10 minutes after collision in a significant wave height of 4 m in following seas is approximately 0.9. These kinds of representations can be used as a base for further statistical analysis.

Simulations were also made for another, symmetrical damage case and for different loading conditions. These simulations were only made in beam seas onto the damage opening. The simulations, as expected, show a larger capsizing resistance as the GM is increased. The capsizing bands of the simulations had some irregularities: in some cases a larger wave height would result in a longer  $T_{cap}$  than for a smaller wave height with the same wave seed. When the time series of these simulations were inspected, it was found that the ship was captured at a list away from the damage for a period of time corresponding approximately to the irregularity of the capsizing band. This is believed to be a plausible physical explanation to the irregularities, made possible by the symmetry of the damage case.

In the final section of the paper, a parameter sensitivity analysis is presented in an effort to assess how well the natural variation in waves needs to be described for accurate results of the capsizing prediction simulations. The results suggest that the minimum of five wave seeds, as stipulated in IMO (1997), may not be sufficient, see Figures 18 and 19.

In conclusion, the calculation procedure presented in this investigation could be used in a wide range of applications such as the development of regulations, in the design process of a ship comparing, e.g., the effect of different internal bulkhead configurations, and possibly be a part of an onboard operational guidance. Further work is needed in areas such as validation of the tool and on the development towards a more comprehensive risk analysis tool.

## ACKNOWLEDGEMENTS

This investigation has been carried out as part of the research project HASARD (Holistic Assessment of Ship Survivability and Risk After Damage). The authors acknowledge the Swedish Governmental Agency of Innovation Systems (VINNOVA) and the Swedish Competence Centre in Maritime Education and Research, LIGHTHOUSE ([www.lighthouse.nu](http://www.lighthouse.nu)), for financing the project.

## REFERENCES

- Dassault Systèmes, (2007). Abaqus/Explicit version 6.7 documentation, analysis users Manual, Section 19.2. Vélizy Villacoublay, France.
- Hogström, P., Ringsberg, J.W. and Johnson, E. (2009). An experimental and numerical study of the effects of length scale and strain state in the necking and fracture behaviours in sheet metal. *International J. of Impact Engineering* **36**(10-11): 1194-1203.
- International Maritime Organization (IMO) (1997). International convention for the safety of life at sea (SOLAS). IMO. London, U.K. IMO Publications.
- International towing tank committee (ITTC). (2002). Specialist committee for the prediction of extreme motions and capsizing. Final report and recommendations to the 23<sup>rd</sup> ITTC. Proceedings of the 23<sup>rd</sup> ITTC. Jersey City, New Jersey, U.S.A. SNAME. 2:619-748
- Jasionowski, A., Vassalos, D. and Guarin, J. (2003). Time based survival criteria for passenger Ro-Ro vessels. *Marine Technology* **40**(4): 278-287.
- Karlsson, U., Ringsberg, J.W., Johnson, E., Hoseini, M. and Ulfvarson, A. (2009). Experimental and numerical investigation of bulb impact with a ship side-shell structure. *Marine Technology* **46**(1):16-26.
- Lee, D., Hong, S.M. and Lee, G-J. (2007). Theoretical and experimental study on dynamic behaviour of a damaged ship in waves. *Ocean Engineering* **34**(1): 21-31.
- Lloyd's Register - Fairplay, (1999 - 2008). *World casualty statistics*. Lloyd's Register - Fairplay Ltd. London, U.K.
- Marine Safety Committee (MSC). (2005). Adoption for the amendments to the international convention for the safety of life at sea, 1974, as amended. MSC194(80).
- Papanikolaou, A., et.al. (2010). GOALDS – Goal Based Damage Stability A New Approach to Passenger Ship Damage Stability and Safety. Proc. 4<sup>th</sup> Intl Conf on Design for Safety, Grado, Italy.
- Schreuder, M. (2005). *Time simulation of the behaviour of damaged ships in waves*. Shipping and Marine Technology. Chalmers University of Technology. Gothenburg, Sweden
- Schreuder, M. (2008). Numerical simulation of foundering scenarios, research study of the sinking sequence of M/V ESTONIA. Gothenburg, Sweden. SSPA.

- Simonsen, B.C., Törnqvist, R. and Lützen, M. (2009). A simplified grounding damage prediction method and its applications in modern damage stability requirements. Marine Structures **22**(1): 62-83.
- Soares, D.G., Jasionowski, A., Jensen, J., McGeorge, D., Papanikolaou, A.D., Pöyliö, E., Sames, P., Skjong, R., Skovbakke Juhl, J. and Vassalos, D. (2009). Risk-based ship design. Editor: Papanikolaou, A. D. Springer-Verlag, Berlin Heidelberg, Germany.
- Spanos, D. and Papanikolaou, A.D. (2007). On the time to capsize of a damaged RoRo/passenger ship in waves. Proc 9<sup>th</sup> International Ship Stability Workshop. Hamburg, Germany.
- Tagg, R. and Tuzcu, C. (2003). A performance-based assessment of the survival of damaged ships: final outcome of the EU research project HARDER. Marine Technology **40**(4): 288-295.
- Vassalos, D. and Jasionowski, A. (2007). SOLAS 2009 – Raising the alarm. Proc of the 9<sup>th</sup> Intl Ship Stability Workshop. Hamburg, Germany.
- Vanem, E., Rusås, S., Skjong, R. and Olufsen, O. (2007). Collision damage stability of passenger ships: Holistic and risk-based approach. Intl Shipbuilding Progress **54**(4): 323-337.